COL10A1 nonsense and frame-shift mutations have a gain-of-function effect on the growth plate in human and mouse metaphyseal chondrodysplasia type Schmid

Matthew S.P. Ho[1], Kwok Yeung Tsang[1], Rebecca L.K. Lo[1], Miki Susic[3], Outi Mäkitie[3,4], Tori W.Y. Chan[1], Vivian C.W. Ng[1], David O. Sillence[5], Raymond P. Boot-Handford[6], Gary Gibson[7], Kenneth M.C. Cheung[2], William G. Cole[3], Kathryn S.E. Cheah[1] and Danny Chan[1,*]

[1]Department of Biochemistry and [2]Department of Orthopaedics and Traumatology, The University of Hong Kong, Pokfulam, Hong Kong, China, [3]Hospital for Sick Children, Toronto, M5G 1X8 Canada, [4]Hospital for Children and Adolescents, University of Helsinki, Helsinki, Finland, [5]Department of Clinical Genetics, The Children's Hospital at Westmead, Westmead, NSW 2145, Australia, [6]Wellcome Trust Centre for Cell-Matrix Research, Faculty of Life Sciences, University of Manchester, Manchester M13 9PT, UK and [7]Bone and Joint Center, ER21015, Henry Ford Hospital, Detroit, MI 48202, USA

Missense, nonsense and frame-shift mutations in the collagen X gene (*COL10A1*) result in metaphyseal chondrodysplasia type Schmid (MCDS). Complete degradation of mutant *COL10A1* mRNA by nonsense-mediated decay in human MCDS cartilage implicates haploinsufficiency in the pathogenesis for nonsense mutations *in vivo*. However, the mechanism is unclear in situations where the mutant mRNA persist. We show that non-sense/frame-shift mutations can elicit a gain-of-function effect, affecting chondrocyte differentiation in the growth plate. In an MCDS proband, heterozygous for a p.Y663X nonsense mutation, the growth plate cartilage contained 64% wild-type and 36% mutant mRNA and the hypertrophic zone was disorganized and expanded. The *in vitro* translated mutant collagen X chains, which are truncated, were misfolded, unable to assemble into trimers and interfered with the assembly of normal α1(X) chains into trimers. Unlike *Col10a1* null mutants, transgenic mice (FCdel) bearing the mouse equivalent of a human MCDS p.P620fsX621 mutation, displayed typical characteristics of MCDS with disproportionate shortening of limbs and early onset *coxa vara*. In FCdel mice, the degree of expansion of the hypertrophic zones was transgene-dosage dependent, being most severe in mice homozygous for the transgene. Chondrocytes in the lower region of the expanded hypertrophic zone expressed markers uncharacteristic of hypertrophic chondrocytes, indicating that differentiation was disrupted. Misfolded FCdel α1(X) chains were retained within the endoplasmic reticulum of hypertrophic chondrocytes, activating the unfolded protein response. Our findings provide strong *in vivo* evidence for a gain-of-function effect that is linked to the activation of endoplasmic reticulum-stress response and altered chondrocyte differentiation, as a possible molecular pathogenesis for MCDS.

INTRODUCTION

In the development of the mammalian skeleton, differentiation and linear growth is mediated by the growth plate cartilage located at the ends of the growing bones via endochondral ossification, a highly coordinated differentiation process during which bone replaces calcified cartilage. This program

---

*To whom correspondence should be addressed. Tel: +852 28199482; Fax: +852 28551254; Email: chand@hkusua.hku.hk

of chondrocyte differentiation, proliferation, maturation and hypertrophy is controlled by a complex network of regulatory molecules and cell–extracellular matrix (ECM) interactions, which, when disrupted results in chondrodysplasia. Metaphyseal chondrodysplasia, type Schmid (MCDS, MIM #156500) is an autosomal dominant skeletal dysplasia. Affected individuals are clinically normal at birth but after they start walking, they develop disproportionate short stature, which is due to progressive shortening and bowing of the femora and tibiae as well as to shortening and sagging of the femoral necks (*coxa vara*). The humeri, radii and ulnae are also shorter but are not bowed, whereas the craniofacial and spinal skeleton are relatively normal (1,2). The shortening and deformities of the long bones are due to impaired function of the thickened and irregular growth plates. Histological studies of a porcine model of MCDS show a thickened and disorganized hypertrophic zone of the growth plate (3).

Individuals with MCDS are usually heterozygous for mutations in the collagen X gene, *COL10A1*. Collagen X is a short chain non-fibrillar collagen produced specifically by hypertrophic chondrocytes (HC) in the hypertrophic zone of mammalian growth plates. Each protein chain consists of a carboxyl-terminal non-collagenous domain (NC1), the main triple helical domain (COL1), an amino-terminal non-collagenous domain (NC2) and a signal peptide. Trimeric molecules of collagen X are assembled from the NC1 domain within the rough endoplasmic reticulum (ER). Strong hydrophobic interactions between the NC1 domains play a critical role in the alignment of the collagen X chains and stabilize the collagen X trimers, ensuring that the triple helix can nucleate and propagate correctly from the C- to the N-terminal end of the molecule. Triple helical molecules of collagen X, containing the terminal NC1 and NC2 domains, are secreted by HC into the ECM.

The *in vivo* impact of MCDS *COL10A1* mutations, comprising missense, nonsense and frame-shift mutations, is poorly understood and both haploinsufficiency and dominant-negative mechanisms have been proposed. In human MCDS, 40 of the 42 reported mutations alter the NC1 domain, whereas two alter the signal peptide cleavage site of the collagen X protein chain (2,4,5). Haploinsufficiency has been implicated in the pathogenesis of human MCDS because mutant mRNAs were absent from the growth plate cartilage of two MCDS patients with nonsense mutations, p.Y632X (6) and p.W611X (7), as a result of premature termination codons. Nonsense-mediated decay of the mutant mRNAs was proposed to be the likely mechanism where the mutant message is preferentially degraded (8), leaving only the wild-type mRNA for translation of reduced amounts of normal collagen X protein chains, which implicates *COL10A1* haploinsufficiency. The two missense mutations altering the signal peptide cleavage site of collagen X were shown, by transfection of heterologous cells, to impair cleavage of the signal peptide and to result in persistent attachment of the mutant collagen X chains to the inner membrane of the ER (9). In these examples it is likely that the mutant collagen X would not be secreted and may similarly result in haploinsufficiency for collagen X.

Haploinsufficiency for collagen X as a mechanism for MCDS is complicated because no true null mutations in *COL10A1* have yet been identified in MCDS, and absence of collagen X in the mouse results in the abnormal distribution of matrix vesicles and matrix components in the growth plates of the null mice (10) and yields a very mild MCDS-like phenotype with late-onset mild *coxa vara*, while heterozygous null mice are phenotypically normal (10). Because the phenotypes of humans with MCDS due to mutations that yield premature termination codons are more severe than that of the collagen X null mouse, it is unclear whether these differences are due to biomechanical and other differences between mouse and man, or whether the human MCDS phenotype is caused by additional mechanisms.

In vitro studies have shown that missense mutations can result in the formation of mutant homotrimers and mixed wild-type and mutant heterotrimers (11–13). In addition, some nonsense or frame-shift mutations (resulting in premature termination codons) of other genes result only in partial degradation of the mutant mRNAs (8,14). Thus, it is possible that *in vivo* interference with the assembly of collagen X acts dominant-negatively resulting in poor or no secretion of mutant homo- and heterotrimers and reduced amounts of normal collagen X in the ECM. In the absence of mutant collagen X in the ECM, the phenotype could be attributed to haploinsufficiency for collagen X. However, if mutant collagen X is secreted to the ECM, there could be a dominant-negative effect on structural properties of ECM. Interestingly, cellular transfection studies have shown that an MCDS *COL10A1* frame-shift mutation p.Y623fsX673, yielding truncated α1(X) chains with a misfolded NC1 domain were retained within the ER, where they stimulated the unfolded protein response (UPR) (15). This finding raises an interesting possibility that even when mutant collagen X is not secreted, *in vivo*, an additional gain-of-function effect could be invoked. The MCDS phenotype may therefore be the outcome of both haploinsufficiency and gain-of-function.

To better understand the molecular mechanisms underlying human MCDS, we investigated the consequences of nonsense and frame-shift mutations of *COL10A1* in *in vitro* protein assembly studies, in human MCDS cartilage and in a transgenic mouse model of MCDS. Mutations that produce human MCDS impaired the *in vitro* assembly of mutant homotrimers as well as the wild-type and mutant heterotrimers. Trimerization of the wild-type molecules was consistently reduced *in vitro* in the presence of the truncated mutant chains. Growth plate cartilage from a proband with MCDS due to a p.Y663X mutation contained wild-type and mutant mRNAs and showed an expanded hypertrophic zone. Assembly of wild-type collagen X *in vitro* was reduced in the presence of the p.Y663X α1(X) chains. Unlike *Col10a1* null mouse mutants, transgenic mice expressing a reported human MCDS mutation, p.P620fsX621, showed an early-onset MCDS phenotype with disproportionate shortening of the limbs and *coxa vara* deformities of the femoral necks. The chondrocyte differentiation program in the growth plate was abnormal and resulted in expansion of the hypertrophic zone. The severity of the latter changes was worse in mice with higher copy numbers and expression of the transgene. These changes correlate with increased levels of Xbp1s (spliced variant of Xbp1), a major transducer of the UPR. These data indicate that if mutant mRNA is available

for translation, the resulting truncated protein is likely to act in a dominant manner with stimulation of the UPR, abnormal regulation of chondrocyte maturation and abnormal architecture and function of the growth plate.

RESULTS

Phenotype of a human metaphyseal chondrodysplasia type Schmid proband

A child (MCDS-18) was identified with typical features of MCDS (2). At 1.5–2 years of age, he developed progressive disproportionate short stature and angular deformities of the legs. By 13 years of age, his height as z-score was -5.7 standard deviations. His limb shortening was rhizomelic in that the proximal portions of his limbs were shorter than the distal portions. His knee, ankle and wrist joints were enlarged. He had a lumbar lordosis due to flexion deformities of his hips; otherwise, his spine was clinically normal. Radiographs showed that the femora and tibiae were bowed and that their growth plates were wider, thicker and less regular than normal (Fig. 1A). A skeletal survey showed similar growth plate changes in the proximal humerii and distal radii, whereas the growth plates of the elbows, hands and spine appeared more normal. Radiographs also showed that the growth plates around the knees temporarily returned to a more normal appearance following surgical realignment of the legs and 6 weeks of non-weight bearing (Fig. 1B). An iliac crest cartilage biopsy from the proband showed that the hypertrophic zone of the iliac growth plate was expanded and that the cellular architecture of the hypertrophic zone was disorganized (Fig. 1C).

P.Y663X mutant mRNA in human metaphyseal chondrodysplasia type Schmid growth plate cartilage

Direct sequencing of the amplified DNA product from exon 3 of the *COL10A1* gene showed that the proband was heterozygous for a c.1989C>G mutation, representing a nonsense mutation, p.Y663X (Fig. 1D). The relative level of normal to mutant *COL10A1* mRNA in the proband's growth plate cartilage, determined by RT–PCR followed by Sfc-I cleavage (Fig. 1E) and single nucleotide extension assay (Fig. 1F), was about 0.64:0.36. The normal to mutant genomic DNA ratios were about 1:1. Therefore, approximately 50% of the expected amount of mutant mRNA was available to be translated into truncated α-chains.

Negative impact of nonsense and frame-shift mutations on *in vitro* collagen X assembly

As the proband's cartilage sample was too small for protein analyses, the assembly of collagen X trimers was quantified in an *in vitro* cell-free translation assay (16). The wt and two normal variant (p.G545R and p.V603M) α-chains had a mean *in vitro* trimerization efficiency of 61.3% (Table 1). In contrast, the p.Y663X mutant α-chains did not produce detectable homotrimers (Fig. 1G). The impact of the p.Y663X α-chains on trimerization of wt α-chains was assessed using wt:mutant transcript ratios of 0.64:0.36, as determined

in vivo. The trimerization efficiency of wt α-chains was significantly reduced from 61.3%, when translated on its own, to 43.8% when it was translated in a 0.64:0.36 ratio with p.Y663X α-chains and further, to 31.5%, when the ratio was 1:1 (Table 1). Similar results were obtained using reporter 'wild-type α1(X) chains' [helixΔ-α1(X)] to better differentiate 'wt' and p.Y663X α-chains (Supplementary Material, Fig. S1).

The quantitative *in vitro* effects of the truncated α1(X) chains produced by the p.W611X and p.Y632X mutations, that were associated with *in vivo COL10A1* haploinsufficiency (6,7), and the effects of the frame-shift p.Y623fsX673 and p.P620fsX621 mutations on wt α1(X)-chain trimer assembly were compared with the results achieved with p.Y663X α1(X)-chains (Fig. 1G and Table 1). The results were similar for all of the truncated mutant α1(X)-chains tested. Thus, if the mutant mRNA is translated, the α1(X)-chains with truncated NC1 domains may have a dominant-negative effect *in vivo* and the impact may be dosage-dependent.

Generation of transgenic mice expressing *COL10A1* metaphyseal chondrodysplasia type Schmid mutation

To address the mechanism for the pathogenesis of MCDS, we produced transgenic mice expressing a mouse *Col10a1* transgene, Cdel, that was equivalent to one of the human frame-shift mutations studied in our *in vitro* protein assembly assay—p.P620fsX621/c.1859delC (17). All transgenes contained a 2 kb 5′-flanking sequence (Fig. 2C) which can direct expression in HC (Tsang, Chan, Cheah, unpublished data). We also created constructs of FColX and FCdel with a Flag® sequence inserted in-frame between Pro[34] and Leu[35] in the NC2 domain in wt and Cdel *Col10a1* vectors, respectively, which allows detection of the Flag®-tagged mutant and wt proteins, respectively (Fig. 2A).

The effect of the Cdel and FCdel α1(X)-chains on mouse collagen X trimerization efficiency was first tested using the *in vitro* assembly assay using equivalent cDNA constructs. Consistent with our results in humans, the mouse wt and FColX α1(X)-chains assembled efficiently into trimers, whereas Cdel and FCdel α-chains failed to produce detectable trimers (Fig. 2B). Co-translation of mouse wt or FColX with FCdel mRNAs did not produce detectable heterotrimers containing wt and FCdel or FColX and FCdel α1(X)-chains. The trimerization efficiencies of mouse wt and FColX α-chains were significantly reduced in the presence of Cdel or FCdel α-chains. The dominant-negative effects of the mouse Cdel and FCdel α1(X)-chains on mouse wt α1(X)-chain assembly were similar to the effects we observed with the equivalent human mutation p.P620fsX621/ c.1859delC (Fig. 1G).

Three FColX founders were generated and all were phenotypically normal (data not shown). Three transgenic founders were generated for each of the Cdel and FCdel transgenes. In two of the three Cdel founders, expression of the transgene was less than 25% of the expression of the endogenous gene. The third founder, which expressed slightly higher levels of the transgene, was selected for the current study. All of the FCdel founders expressed the transgene and one line that expressed the transgene at a level approximately half of the
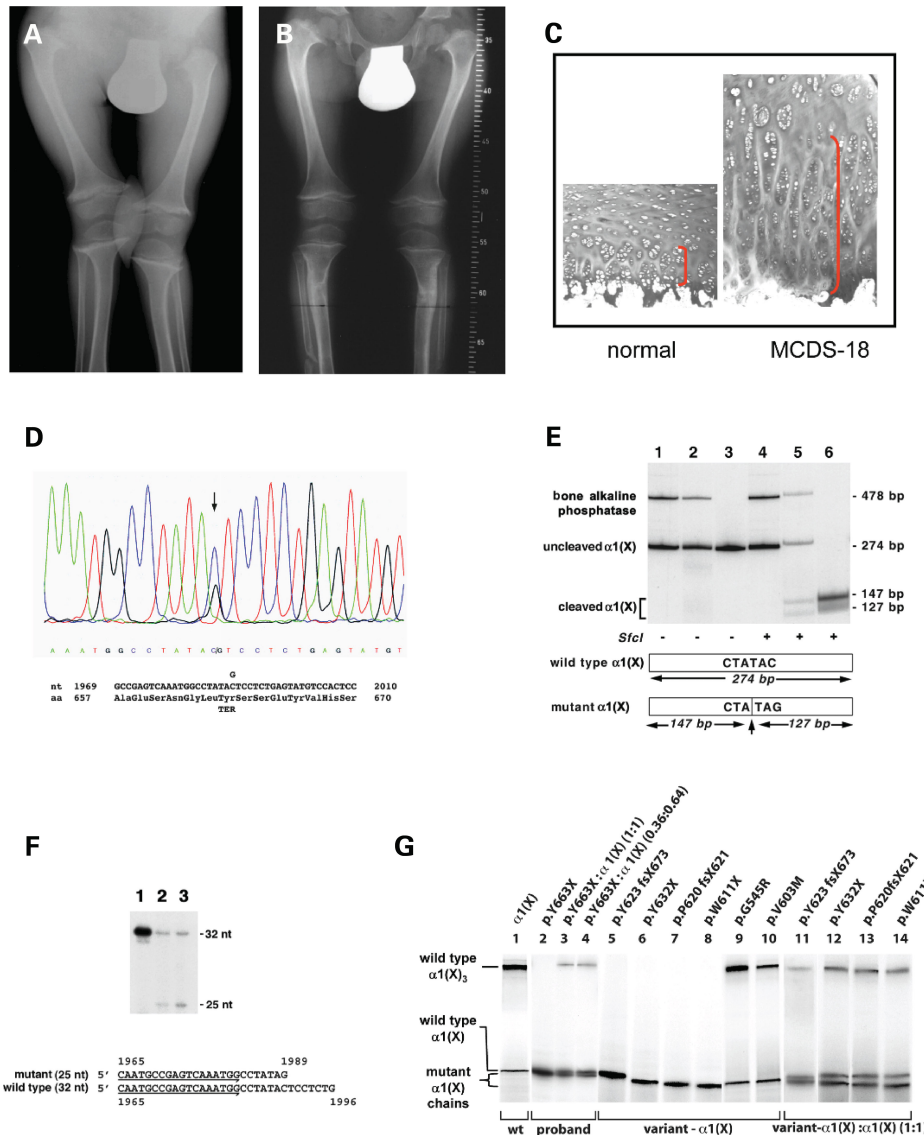
Figure 1. Proband with Schmid metaphyseal chondrodysplasia due to a truncation mutation (p.Y663X) in *COL10A1*. (**A**) Preoperative radiograph at 6 years of age showing valgus deformities of the knees with abnormally thick and irregular growth plates of the distal femurs and of the proximal tibias and fibula. (**B**) Postoperative radiograph taken 6 weeks later showing that surgical realignment of the tibias and bed rest resulted in a more normal appearance of the growth plates above and below the knees. The growth plates returned to their preoperative appearances after a few months of weight bearing. (**C**) Histological analysis of iliac crest growth plates from a normal individual and MCDS patient (MCDS-18), stained with Toluidine blue. (**D**) DNA sequence of the region containing the nonsense mutation. Arrow indicates the nucleotide substitution. The codon change from TAC for tyrosine to TAG for a termination codon (TER) is shown diagrammatically. (**E**) Quantification of wild-type α1(X) and mutant p.Y663X-α1(X) mRNAs in the hypertrophic zone using RT–PCR. Twenty-four cycles of the PCR, which was within the linear part of the yield curve, were used to amplify a 274 bp α1(X) RT–PCR product encompassing the mutation. SfcI digestion was used to differentiate normal and mutant products, as the mutant product contained a novel Sfc1 site yielding two fragments of 127 and 147 bp. A 478 bp bone alkaline phosphatase RT–PCR product was amplified as a marker of HC. The wild-type α1(X) and the bone alkaline phosphatase PCR products were not cleaved by SfcI. PCR products and restriction fragments were resolved by 10% PAGE and quantified by a phosphoimager. *Lanes* 1 and 4, control cartilage; *lanes* 2 and 5, proband cartilage; *lanes* 3 and 6, mutant plasmid p.Y663X-α1(X) cDNA. The products in lanes 4–6 were digested with SfcI (+). In the proband's cartilage sample, 65% of the α1(X) product was wild-type and 35% was mutant. (**F**) Quantification of wild-type α1(X) and mutant p.Y663X-α1(X) mRNAs in the hypertrophic zone using primer extension analysis. Primer extension of the wild-type and mutant templates yielded 32 nt and 25 nt products, respectively. The products were resolved by 10% PAGE and quantified by a phosphoimager. *Lane* 1, wild-type α1(X) cDNA plasmid; *lane* 2, proband hypertrophic cartilage cDNA; *lane* 3, proband genomic DNA. Quantification of the proband genomic DNA showed equal amounts of the wild-type and mutant products while the proband cartilage cDNA showed 36% of the mutant product and 64% of the wild-type product. (**G**) *In vitro* cell-free assembly of human α1(X) chains. Human wild-type [α1(X)], mutant (p.Y623fsX673, p.Y632X, p.P620fsX621, p.W611X and p.Y663X) and polymorphic (p.G545R and p.V603M) cDNA plasmids were used as templates to generate radiolabeled α1(X) chains using the TNT Coupled Reticulocyte Lysate System (Promega), and analyzed on a gradient 4–15% SDS–PAGE. *Lanes* 1, 9 and 10, protein assembly following transcription and translation of individual wild-type and normal variant α1(X) cDNAs. *Lane* 2, Protein assembly of p.Y663X-α1(X) chains. *Lane* 3, protein assembly following co-transcription and translation of a 1:1 mixture of p.Y663X-α1(X) and wild-type α1(X) cDNAs. *Lane* 4, protein assembly following co-transcription and translation of a 0.36:0.64 mixture of p.Y663X-α1(X) to wild-type α1(X) cDNAs. *Lanes* 5–8, protein assembly following transcription and translation of other individual nonsense and frame-shift mutant α1(X) cDNAs. *Lanes* 10–14, protein assembly following co-transcription and translation of 1:1 mixtures of wild-type α1(X) cDNA with mutant α1(X) cDNAs. The migration of monomeric and trimeric chains is shown.

Table 1. Quantitative analysis of trimerization efficiency (%)

	α1(X) Variants (ratio mutant:wt)	N	Mean (%)[a]	SD (%)
Wt and normal variants	wt	49	63.9	9.0
	p.G545R	11	59.3[b]	4.5
	p.V603M	11	60.8[b]	4.2
Nonsense mutations	p.W611X (1:1)	11	35.7[c]	
	p.Y632X (1:1)	5	32.3[c]	7.8
	p.Y663X (1:1)	11	31.5[c]	9.4
	p.Y663X (0.36:0.64)	11	43.8[c]	3.7
Frame-shift mutations with premature termination	p.P620fsX621 (1:1)	11	37.3[c]	9.3
	p.Y623fsX673 (1:1)	11	37.6[c]	7.9

[a]Trimerization of wild-type α1(X) chains determined by densitometry following electrophoresis of the protein products of *in vitro* transcription and translation as shown in Fig. 1G.
[b]No significant differences between wild-type α1(X) and normal variants G545R and V603M α1(X) chains.
[c]Significant reduction in trimerization of the wild type α1(X) chains (ANOVA: degrees of freedom, 8; F, 53.5; $P \leq 0.0001$).
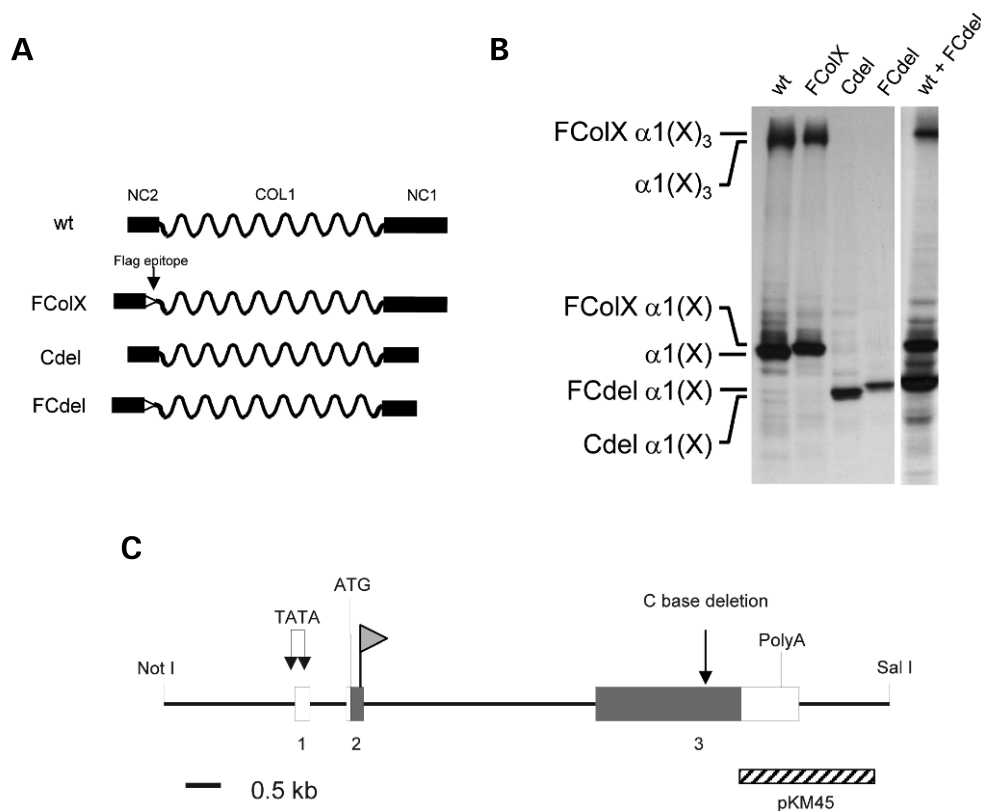

Figure 2. (**A**) The translated products of the mouse transgenes are illustrated, comparing with the wt product. The non-collagenous (NC1 and NC2) and the collageneous (COL1) domains are indicated. (**B**) Cell-free translation demonstrating normal assembly of wt α-chains and FColX α-chains into α1(X)$_3$ and FColXα1(X)$_3$ homotrimers, respectively; but impaired assembly of FCdel and Cdel α-chains into trimers. wt, Wild-type; FColX, Cdel and FCdel are products of FColX, Cdel and FCdel transgenes, respectively. (**C**) Diagrammatic representation of the 10.4 kb *Col10a1* transgene. The exons, key landmarks of the gene and location of the C-base deletion are indicated. The regions coding for the α-chain are shaded and the location of the flag-epitope indicated by a flag in exon 2. pKM45 is a 2 kb fragment of the *Col10a1* gene used as a probe for Southern blot analysis.

endogenous gene was identified. Specific expression of the transgene in HC of FColX and FCdel mice was identified by *in situ* hybridization using a probe containing the Flag® DNA sequence (data not shown), and by immunostaining for the FCdel protein (see below G and H). Since the phenotype of Cdel was mild when compared with FCdel because of the lower transgene expression, FCdel mice were used to evaluate

the impact of differential expression levels of the mutant transgene and the endogenous *Col10a1*. FCdel mice were bred to homozygosity for the transgene, and crossed with *Col10a1*$^{-/-}$ mice (10) that were homozygous for a *Col10a1*-null allele, to generate heterozygous (FCdel$^{+/-}$) and homozygous (FCdel$^{+/+}$) FCdel mice in *Col10a1*$^{+/+}$, *Col10a1*$^{+/-}$ and *Col10a1*$^{-/-}$ backgrounds.
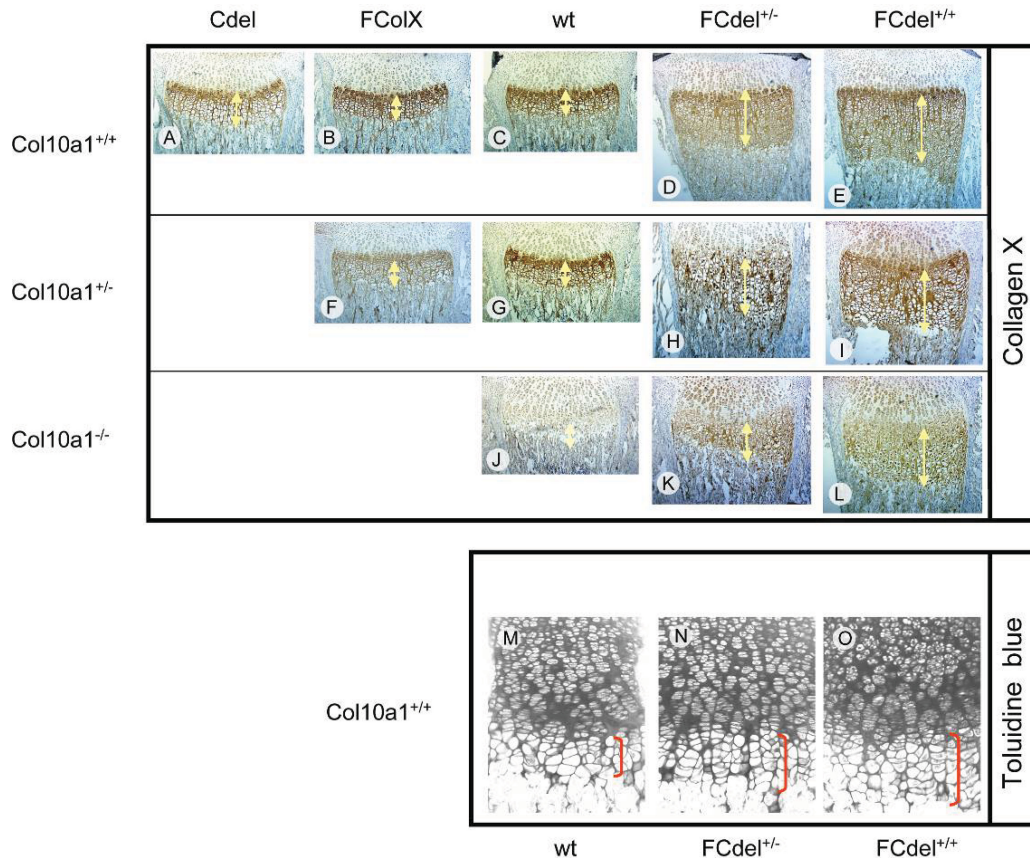
Figure 3. Histological analysis of growth plates from the proximal tibia of wt and transgenic mice stained with an antibody to collagen X (**A**–**L**), and iliac crest growth plates from wt and transgenic mice (**M**–**O**) stained with Toluidine blue. The genotypes of the mice are indicated above and below the figures, and the genetic backgrounds with respective to the endogenous *Col10a1* and *Col10a1*-null alleles are indicated along the left-hand side of the figures. In (**N**) and (**O**), both heterozygous (FCdel$^{+/-}$) and homozygous (FCdel$^{+/+}$) FCdel mice are in a *Col10a1$^{+/+}$* background with two endogenous *Col10a1* alleles. The height of the hypertrophic zone is indicated by double-headed arrows (**A**–**L**), or brackets in (**M**–**O**).

FCdel mRNA available for translation of truncated α-chains

The steady-state level of FCdel mRNA and involvement of the nonsense-mediated decay were determined in homozygous FCdel mice in *Col10a1$^{+/+}$* background, in explant growth plate cultures with and without the addition of cycloheximide. The relative levels of wt and FCdel mRNA were assessed using the protein truncation assay. In the absence of cyclohex-imide, the relative ratio of wt:FCdel mRNA was 1:0.64 $\pm$ 0.28 ($n = 8$). When cultured in the presence of 100 μg/ml cycloheximide for 4 h to protect the degradation of mutant mRNA, the relative ratio of wt:FCdel mRNA increased to 1:1.05 $\pm$ 0.12 ($n = 3$), with a *P*-value = 0.008 when compared with the absence of cycloheximide, indicating that 39% of the mutant mRNA was degraded and 61% available for translation. A representative gel is shown in Supplementary Material, Fig. S2.

Skeletal abnormalities in transgenic mice are consistent with metaphyseal chondrodysplasia type Schmid phenotype

At 5 weeks of age, radiographic measurements of body lengths (BL), from the tip of the nose to the second caudal vertebral centra, did not show any significant differences between FCdel and wt littermates (Supplementary Material, Fig. S3; Table 2), thus the longitudinal growth of the axial and cranio-facial skeleton was normal. However, the long bones of the appendicular skeleton (such as the femora and tibiae) were statistically shorter in all transgenic lines when compared with wt mice. Statistically significant reductions of the ratios of the tibial to BLs were found in all transgenic lines, regard-less of their wt *Col10a1* backgrounds (Table 2). These find-ings confirmed that the FCdel mice had disproportionate shortening of their appendicular skeleton, as observed in human MCDS. The FCdel genotype represents mice that are either heterozygous or homozygous for the *FCdel* transgene, as we did not differentiate these two genotypes in the radio-graphic studies.

A consistent radiographic feature of human MCDS is the development of *coxa vara*, a reduction in the obtuse angle between the femoral neck and shaft (1). At 5 weeks of age, all transgenic lines showed small but statistically significant decreases in their femoral neck-shaft angles, indicating mild *coxa vara* (Supplementary Material, Fig. S3; Table 2). No statistical differences in these angles were detected between the control mouse lines (wt, *Col10a1$^{+/-}$*, *Col10a1$^{-/-}$* and FColX) at this age. *Col10a1$^{-/-}$* mice were previously
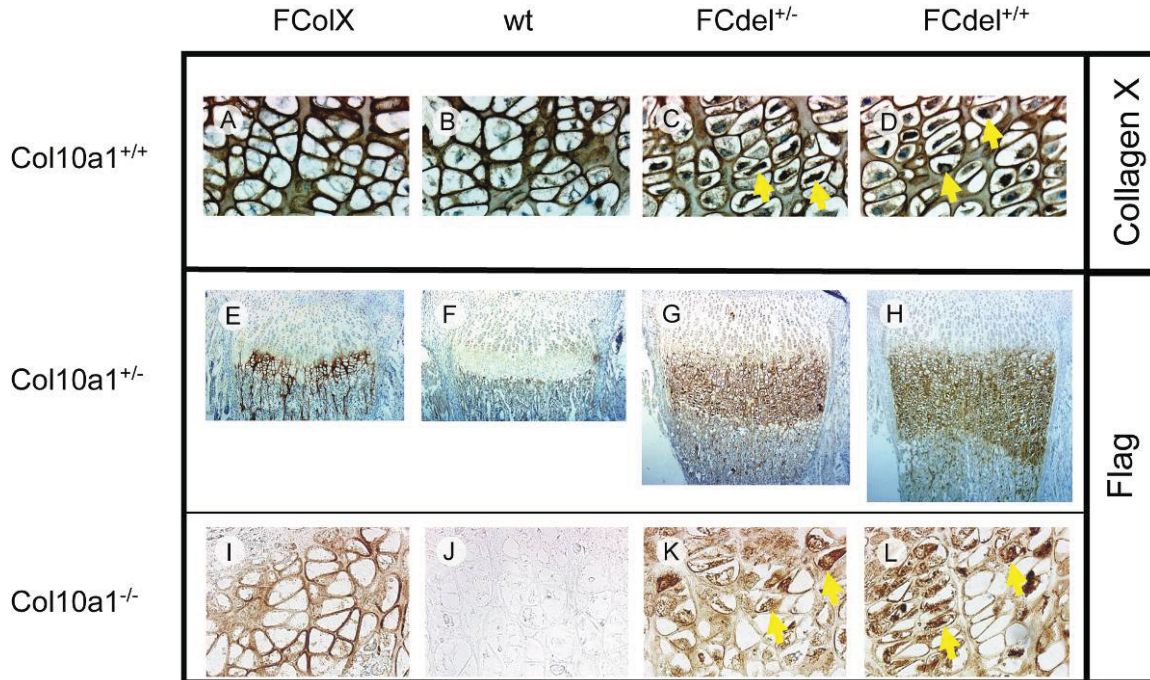
Figure 4. Immunohistological analysis of growth plates from the proximal tibia. (**A**–**D**) High magnification of histological section of growth plates from wt and transgenic mice stained with antibody to collagen X. (**E**–**H**) Low and (**I**–**L**) high magnifications of histological sections of growth plates from wt and transgenic stained with an antibody to the flag epitope. The genotypes of the mice are indicated above the figures, and the genetic backgrounds with respective to the endogenous *Col10a1* and *Col10a1*-null alleles are indicated along the left-hand side of the figures. The arrows indicate a predominant intracellular staining of mutant collagen X, product of the FCdel transgene. High magnification of (**F**), (**G**) and (**H**) is provided in Supplementary Material, Figure S5.

shown to develop late-onset mild *coxa vara* at the age of 15–20 weeks (10).

Expansion of hypertrophic zone in growth plates of Cdel transgenic mice

At 10 days of age, histological analyses of the proximal tibial and distal femoral growth plates were undertaken, as these showed the greatest radiographic change in human MCDS (2). Sections were stained with an antibody to collagen X to highlight the hypertrophic zone (Fig. 3A–L). The distribution of collagen X coincided with the distribution of HC. Similar-sized distinct zones of proliferative and HC were observed in the proximal tibial growth plates of FColX mice, in either *Col10a1*$^{+/+}$ (Fig. 3B) or *Col10a1*$^{+/-}$ (Fig. 3F) backgrounds, and in wt mice (Fig. 3C). These findings indicated that the insertion of the flag-epitope into the NC2 domain did not lead to observable growth plate abnormalities.

Cdel mice in a *Col10a1*$^{+/+}$ background (Fig. 3A) showed a slight but obvious increase in the height of the hypertrophic zone, while FCdel mice in *Col10a1*$^{+/-}$ or *Col10a1*$^{+/+}$ backgrounds had thicker hypertrophic zones (Fig. 3D and E). For transgenic mice in *Col10a1*$^{+/+}$ background, the thickness of the hypertrophic zone was in the order Cdel < FCdel$^{+/-}$ < FCdel$^{+/+}$. Increased expansion of the hypertrophic zones of these transgenic mice was associated with a higher transgene dosage.

Immunostaining showed that collagen X was expressed in the thickened hypertrophic zones of the growth plates of

FCdel$^{+/-}$ and FCdel$^{+/+}$ mice in *Col10a1*$^{-/-}$ backgrounds (Fig. 3K and L). There was no expression of endogenous wt collagen X in these mice so this collagen X was likely to be the truncated Flag® mutant collagen X, a hypothesis supported by positive immunostaining with a Flag® antibody (results not shown). The hypertrophic zone of the FCdel$^{+/+}$ mice was almost twice as thick as that of the FCdel$^{+/-}$ mice in *Col10a1*$^{-/-}$ backgrounds. These findings indicated that the truncated Flag® tagged mutant collagen X protein itself exerted a dosage-dependent gain-of-function effect on the hypertrophic zone in the absence of wt collagen X. The hypertrophic zone of the FCdel$^{+/-}$ was thicker in a *Col10a1*$^{+/-}$ than in a *Col10a1*$^{-/-}$ background (Fig. 3H and K), which suggested that the expressed mutant proteins also exerted a further dominant-negative effect in the presence of wt collagen X. There did not appear to be any additional thickening of the hypertrophic zone in the FCdel$^{+/-}$ mice in a *Col10a1*$^{+/+}$ background when compared with the *Col10a1*$^{+/-}$ background. For the FCdel$^{+/+}$ mice, similar abnormal thickening of the hypertrophic zone was observed in all three *Col10a1* backgrounds (Fig. 3E, I and L), with a trend that is slightly milder in the *Col10a1*$^{-/-}$ background (Fig. 3L). Immunohistological analyses of the growth plates of the distal femora yielded results that were similar to those obtained from the proximal tibiae of the transgenic mice (data not shown).

Growth plate expansion could be detected in FCdel mice from birth (data not shown). By 4 weeks of age, when growth is slowing down as the mice matures and normally the hypertrophic zone is only a layer of few cells, expansion

Table 2. Summary on the skeletal analyses of 5-week-old mice

	wt (n = 23)	Col10a1+/- (n = 13)	Col10a1-/- (n = 32)	FColX (n = 13)[a]	FCdel/Col10a1+/+ (n = 15)[b]	FCdel/Col10a1+/- (n = 22)[b]	FCdel/Col10a1-/- (n = 45)[b]
θ(°)	146.2 ± 5.1	143.5 ± 6.2	143.3 ± 6.1	143.2 ± 6.8	140.4 ± 7.6 ($P = 0.016$)	137.0 ± 6.3 ($P < 0.001$)	137.0 ± 8.0 ($P < 0.001$)
Body length (BL)[c] (mm)	99.4 ± 2.5	101.4 ± 3.4	102.3 ± 4.8	104.5 ± 0.6	100.1 ± 3.1	101.6 ± 3.2	102.6 ± 3.2
Tibia length (TL) (mm)	17.3 ± 0.07	17.5 ± 0.05	17.6 ± 0.07	18.1 ± 0.03	16.1 ± 0.03 ($P = 0.03$)	16.5 ± 0.06 ($P = 0.013$)	16.8 ± 0.04 ($P = 0.004$)
TL/BL ratio	0.174 ± 0.006	0.174 ± 0.007	0.173 ± 0.006	0.174 ± 0.004	0.161 ± 0.004 ($P = 0.004$)	0.163 ± 0.006 ($P = 0.004$)	0.164 ± 0.006 ($P = 0.003$)

[a]Mice in this group are between 5 and 10 weeks of age.
[b]FCdel mice are not distinguished between heterozygous or homozygous status for the transgene.
[c]Body length measured from the tip of the nose to the second caudal vertebral centra.

of the growth plate was marginal when compared with wt mice (Supplementary Material, Fig. S4). Reduced number of collagen X-expressing cells may lessen the impact of the mutant proteins.

Similar expansions of the hypertrophic zones were also observed in iliac crest growth plates from FCdel^{+/-} and FCdel^{+/+} transgenic mice in *Col10a1*^{+/+} backgrounds (Fig. 3M, N and O). These findings were similar to those observed in the iliac crest growth plate of the MCDS proband with the nonsense mutation p.Y663X in the current study when compared with an age-matched control sample (Fig. 1C). In FCdel mice, onset of secondary ossification centers was similar, but there were more hypertrophic cell surrounding the centers (data not shown). No difference in the trabecular bone structure was noted (data not shown).

Transgene product expressed in hypertrophic chondrocytes is retained intracellularly

Immunostaining for collagen X in the hypertrophic zone consistently showed more intracellular staining in FCdel^{+/-} and FCdel^{+/+} mice in *Col10a1*^{+/+} backgrounds than in the wt or FColX mice (Fig. 3). Abundant intracellular collagen X was observed at higher magnification in the HC of FCdel^{+/-} and FCdel^{+/+} mice (Fig. 4A–D). Immunostaining using an antibody specific to the Flag® epitope showed that the FCdel α1(X)-chains were specifically produced by HC (Fig. 4G and H). Most of the FCdel α1(X)-chains were retained within the HC (Fig. 4K and L). Intracellular retention of the FCdel α1(X)-chains was more severe in FCdel^{+/+} (Fig. 4L) than in the FCdel^{+/-} mice (Fig. 4K and Supplementary Material, Fig. S5). The FCdel α1(X)-chains were retained within the ER compartment of the HC, demonstrated by co-localization with immunostained BiP, an ER-resident chaperone (Supplementary Material, Fig. S6). Differences in the pattern of immunostaining with the collagen X and Flag® antibodies in the FCdel^{+/-} and FCdel^{+/+} mice showed that the ECM consisted mainly of wt collagen X.

Intracellular retention of FCdel proteins activates the unfolded protein response

Intracellular retention of misfolded or unfolded proteins can induce ER-stress with activation of the UPR. To determine whether the UPR was triggered in FCdel HC, we studied the expression of key transducers of the UPR. The molecular chaperone, BiP, is up-regulated in the UPR (18) and consistent with the presence of higher levels of unfolded proteins and induction of the UPR, there were more BiP in the HC in FCdel^{+/-} and FCdel^{+/+} mice than in wt littermates, particularly in the lower hypertrophic region (Fig. 5A).

During the UPR, activation of the Perk sensor allows the translation of Atf4, a bZIP transcription factor that induces the expression of the apoptotic gene *Chop/Gadd153* (19,20). The levels of CHOP proteins were higher in FCdel^{+/-} and FCdel^{+/+} than in wt hypertrophic cells (Fig. 5A), but there was no detectable change in the extent of apoptosis in the growth plate (Supplementary Material, Fig. S7). In the wt and FCdel mice, apoptosis occurred at the junction of the hypertrophic zone with the primary trabeculae of the
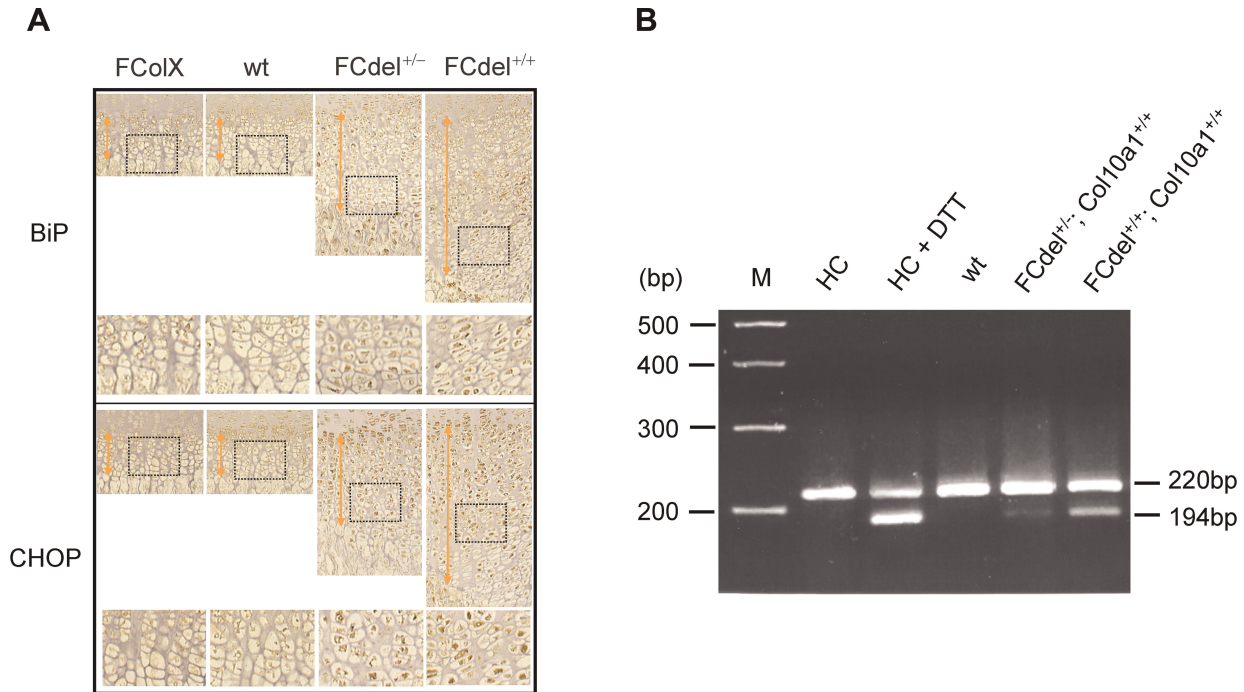
Figure 5. Analysis of gene markers for the activation of ER-stress signaling. (**A**) Immuno-histological analysis of proximal tibia growth plates from wt and transgenic mice stained with specific antibodies to BiP and CHOP (see 'Materials and Methods' section for details). The height of the hypertrophic zone is indicated by double-headed arrows. Note the elevated intracellular staining for both markers in the hypertrophic zone of FCdel$^{+/-}$ and FCdel$^{+/+}$ mice, in a genetic background with two endogenous *Col10a1* alleles. Higher magnifications of the boxed regions are shown under each of the corresponding sections. (**B**) Products of Xbp1 amplified by RT–PCR from extracted mRNA as described in the 'Materials and Methods' section, and analyzed on a 2% agarose gel stained with ethidium bromide. Induction of Xbp1 mRNA splicing in cultured HC with [HC + dithiothreitol (DTT)] and without (HC) DTT treatment was used as a positive control for activation of ER-stress signaling, indicated by the amplification of the 194 bp product (spliced variant of Xbp1). The product from the unspliced variant of Xbp1 is 220 bp. Indication of ER-stress signaling (194 bp product) is also noted in RT–PCR products amplified from mRNA extracted from growth plate cartilage of heterozygous (FCdel$^{+/-}$) and homozygous (FCdel$^{+/+}$) FCdel mice in genetic backgrounds with two endogenous *Col10a1* (Col10a1$^{+/+}$) alleles, which is absence in wild-type (wt). (**M**) DNA marker from Amersham.

metaphysis. We investigated whether the degree of UPR activation corresponded with transgene dosage by looking at the splicing of *Xbp1*, a downstream responsive gene of the stress sensor, Ire1. The alternative transcript *Xbp1^s* is generated by an unconventional splicing of 26-nt from *Xbp1* mRNA by activated *Ire1*. It contains a translational frame-shift and encodes a potent transcription factor that activates UPR-inducible genes (18,21,22). The levels of the two *Xbp1* transcript isoforms in FCdel$^{+/-}$, FCdel$^{+/+}$ and wt mice were monitored by RT–PCR of mRNA extracted from the growth plate cartilage. Wild-type HC yielded only the unspliced transcript under normal conditions. As a positive control, ER-stress induced by the addition of dithiothreitol (DTT) yielded both the spliced and the unspliced transcripts (Fig. 5B). Both transcripts were present in FCdel$^{+/-}$ and FCdel$^{+/+}$ samples (Fig. 5B), but the spliced transcript was more abundant in the FCdel$^{+/+}$ samples, indicating that the level of UPR activation of *Ire1* correlated with transgene dosage.

Altered gene expression profile of terminal differentiated hypertrophic chondrocytes in FCdel mice

We hypothesized that the observed expansion of the hypertrophic zone was due to impaired terminal differentiation of FCdel$^{+/+}$ and FCdel$^{+/-}$ HC. As wt proliferating chondrocytes

enter and progress through hypertrophy, several genes are characteristically changed in preparation for the conversion to bone (23,24). For example, *Ppr* is expressed predominantly by pre-hypertrophic cells and are down-regulated as cells enter hypertrophy (Fig. 6A), while *Opn* is expressed by terminally differentiated HC at the chondro-osseous junction (Fig. 6D). Consistent with a disruption of differentiation of terminal HC, while *Ppr* was down-regulated in the upper hypertrophic zone in FCdel$^{+/-}$ (Fig. 6B) and FCdel$^{+/+}$ (Fig. 6C) mice, it was expressed at a higher level again in some cells nearer to the chondro-osseous junction, in contrast to its persistently decreased expression in the wt hypertrophic zone. Furthermore, the expression of *Opn* is no longer restricted to the terminal layer of the HC in FCdel$^{+/-}$ (Fig. 6E) and FCdel$^{+/+}$ (Fig. 6F) mice. The expression of *Col10a1*, which was even throughout the wt hypertrophic zone (Fig. 6G), was reduced in the lower hypertrophic zone in FCdel$^{+/-}$ mice (Fig. 6H). The reduction in *Col10a1* expression was greater in the FCdel$^{+/+}$ mice (Fig. 6I) than in the FCdel$^{+/-}$ mice (Fig. 6H).

DISCUSSION

The present study was undertaken to investigate the mechanisms operating *in vivo* in the pathogenesis of MCDS resulting from the introduction of premature termination codons into the
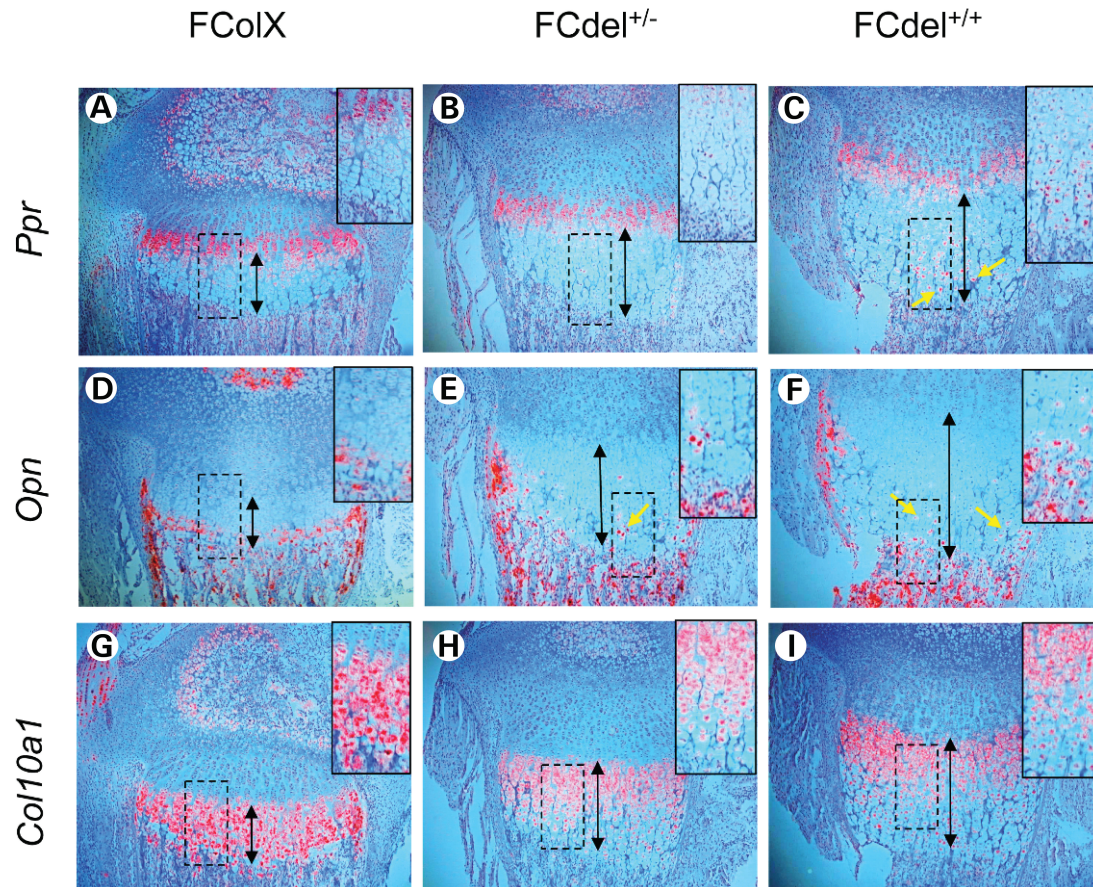
Figure 6. Analyses of the proximal tibial growth plate of 10-day-old mice. *In situ* hybridization for *Ppr* (**A**–**C**), *Opn* (**D**–**F**) and *Col10a1* (**G**–**I**). Expression in heterozygous (FCdel$^{+/-}$) and homozygous (FCdel$^{+/+}$) FCdel mice is compared with FColX mice all in *Col10a1$^{+/+}$* background. The inserts in (**B**) and (**C**) are higher magnifications of the boxed region of the corresponding panel. The hypertrophic zone is marked with a double-headed arrow, and cells abnormally expressing *Ppr* and *Opn* in the lower hypertrophic zone of FCdel$^{+/+}$ mice indicated with yellow arrows.

region of the *COL10A1* transcript that encodes the NC1 domain of α1(X) collagen chains. By *in vitro* protein assembly assays, analysis of human MCDS tissue and mouse models, we have provided *in vivo* evidence that MCDS *COL10A1* mutations, while resulting in some mRNA degradation, also exerted a gain-of-function effect on the growth plate which results in chondrodysplasia.

The proband MCDS-18, in the current study, was heterozygous for a p.Y663X mutation that produced truncated α1(X) chains lacking the last 18 amino acids of the NC1 domain. Iliac crest growth plate cartilage from the proband contained approximately 64% wt and 36% p.Y663X α1(X) mRNAs. We estimated that approximately 50% of the mutant mRNA was degraded, while the rest was translated into truncated α1(X) chains. Because the iliac crest cartilage sample was too small for protein analyses, we investigated the impact of these truncated chains in *in vitro* protein assembly assays.

These assays showed that the proband's p.Y663X α1(X)-chains did not form stable homotrimers and were unable to form stable heterotrimers with wt α1(X)-chains. Similar findings were observed for p.W611X and p.Y632X α1(X)-chains but these chains are not produced in human MCDS growth plate cartilage because of nonsense-mediated

decay of the mutant mRNA (6,7). Two human MCDS frameshift mutations, p.Y623fsX673 and p.P620fsX621, similarly impaired trimer assembly although it is unknown whether mutant proteins were synthesized *in vivo* (16). The proband and reported mutations, included within the current study, truncated the last β-strand H of the NC1 domain, which is normally buried within the interior of the domain (25). From the crystal structure, truncations within the β-strand H were predicted to prevent the folding of the NC1 subunits and their assembly into trimers, however, our current and previous *in vitro* assembly studies showed that the truncated α1(X)-chains interfered in a dominant-negative manner with the assembly of wt trimers. Although we did not identify the proximal interacting peptide sequences, it is likely that the interactions between the wt and mutant chains involved the conserved aromatic motif (26) F^{589}–Y^{601} within the NC1 domain. This motif, which is probably the initial site of interaction and registration of the α1(X)-chains, has been shown to be critical for the assembly of trimers (11).

It was of interest to note that while the mutant chains were unable to form 'stable' trimers, their presence in co-translation studies showed a negative effect on the efficiency of wt chain trimerization. The wt trimers that can be detected are held

together by stronger hydrophobic interaction via the NC1 domain (16). Thus, the negative effect is likely to result from 'unstable/non-productive' interactions between wt and mutant chains that cannot be detected using SDS–PAGE, and the effect is a reduced pool of wt chains forming stable trimers, consistent with a dominant-negative mechanism in which mutant α1(X) chains interferes with wild-type collagen X assembly.

Previous transfection studies provided insights into the disease mechanisms that may occur *in vivo* if HC synthesized α1(X) chains with truncated NC1 domains. Transient transfections of heterologous cells with the frame-shift mutations p.Y623fsX673 and p.P620fsX621 yielded small amounts of mutant α1(X) collagen chains that were retained within the cells (16). The truncated α1(X) chains were sensitive to limited pepsin digestion, indicating that they were unable to form correctly assembled triple helical collagen X molecules (16). Stable transfection of the p.Y623fsX673 mutation in heterologous cells confirmed that the mutant collagen chains were retained with the cells (27,28). Cells expressing these mutant α1(X) chains had significantly increased amounts of BiP and the spliced form of Xbox DNA-binding protein mRNA (Xbp1), two key markers of the UPR (18,29).

Our analysis of the transgenic FCdel mice, bearing the mouse equivalent of the human MCDS p.P620fsX621 mutation, while confirming previous *ex vivo* findings also provide new insights into the pathogenesis of MCDS. Our results indicated that HC specifically expressed the transgene and that approximately 60% of the mutant mRNA escaped nonsense-mediated mRNA decay, similar to the human MCDS-18. The FCdel α1(X) chains that lacked the C-terminal 60 amino acids of the NC1 domain were synthesized by the HC but the protein accumulated within the ER. Retention of the FCdel α1(X) chains was associated, in a concentration-dependent manner, with increased thickness and abnormal maturation of the hypertrophic zone. Thickening of the hypertrophic zones of the FCdel$^{+/-}$ and FCdel$^{+/+}$ mice, in the absence of endogenous collagen X, indicated that the retained protein exerted a gain-of-function, activating ER-stress signaling affecting growth plate maturation. The increase in thickness of the hypertrophic zone of the FCdel$^{+/-}$ mice in the *Col10a1*$^{+/-}$ background when compared with the *Col10a1*$^{-/-}$ background was probably due to the additional negative impact of the FCdel α1(X)-chains on the assembly of endogenous collagen X trimers, as observed in our *in vitro* protein assembly assay. It is likely that impaired trimerization of the wt α1(X) chains resulted in the retention of unassembled wt α1(X) chains in the ER along with the FCdel α1(X) chains, increasing the pool of unfolded/unassembled proteins, influencing the level of ER-stress. Unfortunately, we were unable to show increased intracellular wt chains experimentally because while the Flag antibody was able to specifically identify the FCdel α1(X) chains in the ER, our collagen X antibody was unable to distinguish the wt α1(X) chains from the FCdel α1(X) chains in the ER.

Previous studies of *Col10a1*-null mice showed that the absence of collagen X in the ECM did not result in abnormal chondrocyte maturation (10). Consequently, the abnormal hypertrophic chondrocyte maturation observed in the FCdel mice probably resulted from the adverse effects of the

mutant protein retained within the ER. In agreement with previous transfection studies, the retained FCdel α1(X) chains activated an ER-stress response.

Activation of ER-stress responses due to protein misfolding has been implicated in the pathogenesis of many diseases [see review by (30)]. In FCdel mice, the HC had elevated levels of BiP, Chop and Xbp1^s, which are key markers of ER-stress. Xbp1^s is a potent transcription factor and is known to be correlated with the level of ER-stress (31,32). Its expression in the FCdel mice showed that the level of ER-stress increased with transgene dosage. In the FCdel mice, ER-stress due to retained misfolded α1(X) chains appeared to be the cause of the abnormal differentiation of the hypertrophic cells, thickening of the hypertrophic zone and impaired longitudinal bone growth. Hypertrophic cells in the upper part of the hypertrophic zone expressed typical phenotypic markers. However, rather than undergoing apoptosis, as observed in wt growth plates, the hypertrophic cells persisted. The phenotypic changes at the lower hypertrophic zone included down-regulation of *Col10a1* and the upregulation of *Ppr*. This together with a disrupted expression of *Opn* at the chondro-osseous junction is consistent with the notion that activation of ER-stress signaling has altered chondrocyte differentiation. Previous studies had shown that ER-stress resulted in the loss of differentiation of cultured chondrocytes (33). Xbp1^s, which can play a role in cellular differentiation (34,35), may provide the link between ER-stress and altered chondrocytic differentiation.

The FCdel mice showed early-onset disproportionate shortening of their appendicular skeleton relative to their axial and craniofacial skeletons. Similar early-onset disproportionate shortening of the limbs was reported in the human bearing the same p.P620fsX621 mutation (17) as well as in our current proband with a p.Y663X mutation. Early-onset *coxa vara* was also observed in the FCdel mice and in the probands with the p.P620fsX621 and p.Y663X mutations. However, radiographs of the FCdel mouse femora and tibiae neither showed the thickened and irregular growth plates nor the metaphyseal and diaphyseal bowing that was observed in the legs of the probands with the p.P620fsX621 and p.Y663X mutations. These findings suggested that the lower limb phenotype was more severe in the human probands than in the FCdel mice. The severity of the radiographic changes in the human probands appeared to be related to weight bearing and to the intrinsic growth rates of the different growth plates. For example, the non-weight bearing arms did not show any bowing of the long bones. Thickening and irregularity of the growth plates were observed in the fast growing proximal humeri and distal radii but not in slow growing distal humerii, hands or in the proximal radii and ulnae. The adverse effects of weight bearing were likely to account for the post-natal onset of leg deformities and for the more severe radiographic changes in the legs than in the arms. The radiographic appearance of the distal femora and proximal tibiae were modulated in proband MCDS-18 by realignment surgery and 6 weeks of non-weight bearing. During this 6-week period, the growth plates around the knees became normal in thickness and developed a well-defined metaphyseal layer of trabecular bone but reverted to their preoperative appearances after the resumption of weight bearing.

The mechanisms involved in these changes are unknown but may involve the modulation of differentiation of the hypertrophic zone. It is probable, based on the findings in the FCdel mouse that weight bearing adds to the stress, leading to thickening of the hypertrophic zone with abnormal differentiation of the HC and delayed endochondral bone formation. Removal of the weight bearing reduces stress, enabled differentiation to proceed more normally, and a more 'normal' transition to the trabecular bone in the metaphysis.

Collagen X null mice have mild *coxa vara*, one of the many characteristics of MCDS (10), and it is late-onset in contrast to the early-onset, moderate form of MCDS in the FCdel mice. This supports a dominant mechanism for MCDS mutations, which disrupts collagen X assembly as opposed to complete absence of protein. Similar differences may also apply to humans with MCDS depending on whether mutant $\alpha 1(X)$ chains are synthesized or not. The proband in the present study had the clinical onset of MCDS at the early age of 1.5–2 years. It is likely that the severity and age of onset of this MCDS reflected the dominant effects of the p.Y663X $\alpha 1(X)$ chains. The proband with the mutation that was used to create the FCdel mice was reported also to have typical MCDS with similar onset at about 2 years of age and similar radiographic severity to our proband. In contrast, the reported probands with *COL10A1* haploinsufficiency due to p.Y632X (6) and p.W611X (7) mutations presented at 11 and 7 years of age, respectively. It is not clear whether the patients with early or late clinical onset of their MCDS differ in their ultimate severity of short stature and deformities. Additional cases and further studies would be needed to clarify this point.

MATERIALS AND METHODS

Analysis of iliac crest growth plate cartilage samples from an metaphyseal chondrodysplasia type Schmid patient with a p.Y663X mutation

A block of iliac crest apophyseal growth plate cartilage, approximately 5 mm wide and 5 mm deep, extending from its superior tendinous surface to the underlying trabecular bone of the pelvis was obtained from a 13-year-old proband (MCDS-18) with MCDS during hip reconstructive surgery. Similar tissue was obtained from four individuals of similar ages during the harvesting of iliac bone grafts for orthopedic procedures. The latter individuals did not have skeletal dysplasias or disorders that were likely to affect the growth plate of the iliac crest. Blood was also taken from the proband for the preparation of genomic DNA. All samples were obtained with informed consent approved by the Institution's Human Ethics Committee. The tissues were embedded in paraffin after decalcification in EDTA. Sections of 5 μm were processed for histological analysis.

Genomic DNA was extracted from whole blood using QIAmp DNA Blood Mini Kit (Qiagen) for PCR amplification of the *COL10A1* gene for sequencing. mRNA was prepared using the Dynabeads mRNA Purification Kit (Dynal) from total RNA extracted from frozen sections of the hypertrophic zones of iliac crest cartilage samples using the Trizol reagent (Invitrogen). The relative levels of normal and mutant collagen X mRNA were determined by RT–PCR followed by restriction mapping or primer extension with nucleotide-specific chain termination.

For RT–PCR, reverse transcription was performed using oligodT as primer. Primers 5′-GCCTGTATAAGAATGGCACC-3′ (nt 1838–1857) and 5′-GTAGGGTGGGGTAGAGTTAG-3′ (nt 2092–2111) were used for the amplification of *COL10A1* cDNA. As an internal control, alkaline phosphatase cDNA was amplified using primers 5′-ATGAAGGAAAAGCCAAGCAG-3′ (nt 1022–1041) and 5′-GCAGGAGCACAGTGGCCGAG-3′ (nt 1480–1499). The reverse primers were end-labeled with $[\gamma\text{-}^{32}\text{P}]$-ATP (Amersham) and T4 kinase (New England Biolabs). PCR amplification was optimized for quantification. Normal and mutant PCR products were differentiated by digestion with *Sfc*-I (New England Biolabs) and quantified using a phosphoImager 400E (Molecular Dynamics) and ImageQuant Software version 3.3 (Molecular Dynamics) and visualized by autoradiography.

For primer extension with nucleotide-specific chain termination, a primer 5′-CAATGCCGAGTCAAATGG-3′ (nt 1965–1982) end-labeled with $[\gamma\text{-}^{32}\text{P}]$-ATP and T4 kinase, was the extended proband's genomic DNA and a 274 bp RT–PCR product as templates. The 274 bp RT–PCR product contains the mutation and was obtained following 24 cycles of PCR, which is within the linear part of the product–yield curve. The primer was extended using the Sequenase Version II DNA Polymerase (Amersham) and a nucleotide mixture containing 2.5 mM dTTP, 2.5 mM dATP, 2.5 mM dCTP and 2.5 mM ddGTP. The extended products were resolved on a 10% denaturing polyacrylamide gel, and radioactive fragments quantified using a PhosphorImager 400E (Molecular Dynamics).

Mouse *COL10A1* mutagenesis

A human MCDS mutation, c.1859delC (4,17), was created at the equivalent site in the mouse *Col10a1* gene by site-directed mutagenesis using overlapping PCR as previously described (36). Given that the mouse sequence differs from the human sequence around the region of the C base deletion, a primer, 5′-TGTATAAGAATGGCACCCTG*TAA*TGTACAC-3′, corresponding to the human sequence was used to introduce the mutation, to produce the predicted outcome of p.P620fsX621 (17), representing a frame-shift at amino acid position 620, followed with a termination codon, TAA (italicized in the primer sequence), at position 621. The resultant Cdel $\alpha 1(X)$ chain is shorter by 60 amino acids.

The PCR product containing the mutation was cloned into a 10.5 kb fragment of the mouse *Col10a1* gene to generate the *Cdel* transgene containing 2 kb of the 5′- and 1.3 kb of 3′-flanking sequence after exon 3 (Fig. 2C). The Cdel mutation was also created in a Flag-epitope-tagged *Col10a1* gene (*FColX*) to produce the *FCdel* transgene. *FColX* transgene contains the Flag-epitope sequence (5′-GACGACGATGACAAGCTTGCGGGCCCA-3′) inserted in-frame into exon 2 at nucleotide position 741 (numbered from the start of transcription) of the mouse *Col10a1* gene (Fig. 2A).

Generation and genotyping of transgenic mice

Cdel, FCdel and FColX transgenic mouse founders were generated by pronuclear injection of *Cdel*, *FCdel* and *FColX* transgenes, respectively, into one-cell CBA/C57BL6 F1-hybrid zygotes using standard protocols (37). FCdel and FColX transgenic mice were mated with F1 mice (CBA/C57BL6) for several generations to produce mice containing a single integration site for the transgene, and these mice were used in all subsequent analyses. FCdel and FColX transgenic mice were crossed with *Col10a1*$^{-/-}$ mice (10) containing null alleles for the *Col10a1* gene, to produce compound heterozygous, which were inter-crossed to produce FCdel and FColX transgenic mice in *Col10a1*$^{+/+}$, *Col10a1*$^{+/-}$ and *Col10a1*$^{-/-}$ genetic backgrounds. FCdel mice in the different endogenous *Col10a1* backgrounds were further inter-crossed to produce mice that are heterozygous (FCdel$^{+/-}$) or homozygous (FCdel$^{+/+}$) for the *FCdel* transgene.

Mice were genotyped from tail biopsy DNA by allele-specific PCR using a sense primer 5′-ATGCCTGATGG CTTCATAAA-3′ and a mutant-specific antisense primer 5′-CTCATCATACGTGTACATTAC-3′. In some cases, genotyping was also performed by restriction enzyme digestion as the mutation (c.1859delC) results in an additional *Ban*-I site. Mice containing the Flag-epitope were genotyped using primers, 5′-GAAACAGATCAGTGATG GGCTA-3′ and 5′-GCGTATGGGATGAAGTATTGTG-3′, to amplify a region of the gene flanking the Flag-epitope with a product size difference of 36 bp, corresponding to the Flag-epitope sequence. The *Col10a1*-null allele was identified by the amplification of a 0.5 kb PCR product using a sense primer, 5′-AGGGGAGGAGTAGAAGGT-GG-3′, which anneals to the *pgk* promoter of the pgkNeo cassette, and an antisense primer, 5′-ATACCTTCTCGTCCTTGCTT-3′, to *Col10a1*. The endogenous *Col10a1* allele was identified by a 1.5 kb fragment amplified using a sense primer, 5′-CCATATGGACACAAAGGAGATATT-3′, and an anti-sense primer, 5′-CATCATACGTGTACATCGTAG-3′, that will not prime to the *Cdel/FCdel* transgenic alleles. In the latter reaction, the amplification of the *Col10a1*-null allele was excluded by limiting the extension time in each cycle of the PCR.

Southern blot analysis

The number of transgenes integration site(s) in the transgenic founders/lines were analyzed by Southern blot analysis using *Bam*-HI-digested genomic DNA hybridized with a [α-^{32}P]-dCTP labeled 2073 bp probe (Fig. 1D) derived from the *Bam*-HI/*Eco*-RI fragment (residue 5642–7679, numbered from the start codon) of the mouse *Col10a1* gene. This probe will hybridized to a 10.0 kb Bam-HI fragment of the endogenous *Col10a1* gene and variable bands of Bam-HI fragment (>2 kb) depending on the integration site(s) of the transgene.

Detection of mRNA expression in mouse cartilage by RT–PCR

Total RNA was extracted from growth plate cartilages of limb bones from 10-day-old mice. For the detection of mRNA of the endogenous *Col10a1* gene, and the *Cdel* or *FCdel* transgenes, reverse transcription was performed using the reverse transcriptase, Superscript II (Invitrogen Corp.), and a specific 3′ antisense primer, MH2–MX 5′-GGGCTTTAGGGATTG CTGAGTG-3′, complementary to the 3′-region of the *Col10a1* mRNA. PCR amplification of the cDNA was performed using three primers, a sense primer MH3–MX (5′-ATGCCTGATGGCTTCATAAA-3′), another sense primer MH1–Cdel (5′-ATAAGAATGGCACCCTGTAA-3′), and anti-sense primer of MH2–MX in a PCR reaction with the addition of 1.6% (v/v) formamide. The MH3–MX and MH2–MX primer set will amplify a 0.7 kb fragment, representing the endogenous *Col10a1* transcripts, and the MH1–Cdel and MH2–MX primer set amplifies a 419 bp fragment, representing the mutant transcript as MH1–Cdel is specific for the Cdel mutation.

The expression level of Xbp1 and a spliced variant, Xbp1^{s}, induced by the UPR was also determined by RT–PCR from total RNA extracted from growth plate cartilages of limb bones from 10-day-old mice. Reverse transcription was performed using oligo-dT. Thirty cycles of PCR were then performed (94°C for 30 s, 58°C for 30 s and 72°C for 90 s) using sense 5′-GATCCTGACGAGGTTCCAGA-3′ (residues 434–453) and antisense 5′-ACAGGGTCCAACTTGTCC AG-3′ (residues 652–634) primers for Xbp-1 cDNA, and the amplicons analyzed on a 2% (w/v) NuSieve low-temperature melting agarose (FMC) gel-stained with ethidium bromide.

Radiological analysis for metaphyseal chondrodysplasia type Schmid characteristics in mice

Radiological images were taken for 5- and 10-week-old mice. All images were taken under identical exposure and radiation energy (24 kV/25 mA) using high-resolution Kodak mammography X-ray film (Kodak Diagnostic film Min-R™ H MRH-1), and a General Electric X-ray machine (Senograph 600T Senix HF, General Electric, USA). Mice were anaesthetized to facilitate radiography and all were positioned such that the greater trochanters of both femurs were clearly seen on the radiographs. On the radiographs, axes for the femur neck and shaft were drawn, and the obtuse angles between these two axes were measured as previously described (10). The BL of each mouse was measured from the tip of the nose to the second caudal vertebral centra. Tibial bone length was also measured. Measurements were analyzed for statistical differences by the Mann–Whitney's *U* test and a two-tailed *P*-value <0.05 is taken as statistically significant.

Histochemistry and immunohistochemistry

Limbs were fixed in freshly prepared 4% (w/v) paraformaldehyde, and demineralized in 0.5 M EDTA (pH 7.5) for 24 h prior to embedding in paraffin. Histochemistry (toluidine blue and H&E) and immunohistochemistry was performed on 5 μm dewaxed sections. The second antibody-HRP-conjugated polymer system (EnVision+, Dako) was used to detect antibodies to BiP (1:250; Stressgen), CHOP (1:200; Santa Cruz), Collagen X (1:500; from Dr Olena Jacenko, University of Pennsylvania, USA) and Flag (1:1600; Sigma). For collagen X and Flag antibody staining,

sections were digested with 0.8% (w/v) type-II hyaluronidase (Sigma) at 37°C for 30 min before serum-blocking and application of the antibodies. Sections were counter-stained with hematoxylin.

In situ hybridization

In-situ hybridization was performed as previously described (38), using [^{35}S]UTP-labeled riboprobes for *Col10a1* and *Col2a1* (38), the *PTHrP* receptor (*Ppr*) and *Opn* (from H. Kronenberg).

Cell-free translation and *in vitro* trimer assembly

A plasmid pFX1, containing the full-length human collagen X cDNA was used as a template to generate the mutant plasmids Y623fsX673, Y632X, P620fsX621 and W611X, as well as the polymorphisms G545R and V603M. The mutations were amplified from patient genomic DNA, and sub-cloned into pFX1. Transcription and translation were performed using the TNT-coupled transcription and translation system (Promega) to assess trimerization, as previously described (16). The translated products were analyzed using a 4–15% SDS–PAGE (Criterion gels, BioRad). Mouse wt, FColX, Cdel and FCdel full-length cDNA constructs were generated in pBluescript II SK (−) (Stratagene). Expression and trimerization were similarly assessed using the TNT-coupled transcription and translation system (Promega) (16), and the translated products analyzed using a 7.5% (w/v) SDS–PAGE. [^{35}S]-Met-labeled proteins quantified using a phosphorImager 400E (Molecular Dynamics).

Protein truncation test

Cell-free transcription and translation was also used to rapidly screen for homozygous *FCdel* transgenic mice in different backgrounds for the endogenous *Col10a1* allele using the protein truncation test (PTT) by comparing the *FCdel* transgene copy number relative to the endogenous *Col10a1* gene. This method was originally designed for rapid screening of truncation mutations in patients by Roest *et al.* (39), and modified by Bateman *et al.* (40) for quantitative analysis of *COL10A1* mRNA level with nonsense mutations. For analysis of FCdel mice, a 1.5 kb DNA fragment including the region of Cdel mutation was amplified from both the endogenous *Col10a1* and the *FCdel* transgene using a sense primer, 5′-GC**TAATACGACTCACTATAG**GAACAGACCACC*A-TG*AAGCAAGGACGAGA-AGGTAT-3′, and an antisense primer, 5′-GATGAGCTTGACAGG-AAGTGC-3′. The sense primer contains sequence for the T7 promoter (indicated in bold), and the ATG start codon (indicated in bold and italics) in-frame with the coding sequence to be amplified from exon 3. The antisense primer is 3′ of the stop codon for *Col10a1*. The PCR products were transcribed and translated using the TNT-T7 polymerase-coupled transcription and translation system (Promega) as described above. The [^{35}S]-methionine-labeled products were resolved by SDS–PAGE and imaged using the PhosphorImager (Molecular Dynamics). The 40 kDa (product from the endogenous *Col10a1* allele) and 34 kDa (product from the FCdel

transgene) products were quantified and their relative ratio determined following adjustment of the number of methionine residues, to identify mice that are heterozygous or homozygous for the *FCdel* allele. This method was also used to estimate the copy number of the transgene, and for determining the relative levels of wt and FCdel mRNA in explant cultures in the presence or absence of 100 μg/ml cycloheximide (Sigma Chemical Co., St Louis, MO, USA).

SUPPLEMENTARY MATERIAL

Supplementary Material is available at HMG Online.

REFERENCES

1. Lachman, R.S., Rimoin, D.L. and Spranger, J. (1988) Metaphyseal chondrodysplasia, Schmid type. Clinical and radiographic delineation with a review of the literature. *Pediatr. Radiol.*, **18**, 93–102.
2. Makitie, O., Susic, M., Ward, L., Barclay, C., Glorieux, F.H. and Cole, W.G. (2005) Schmid type of metaphyseal chondrodysplasia and *COL10A1* mutations-findings in 10 patients. *Am. J. Med. Genet. A*, **137**, 241–248.
3. Nielsen, V.H., Bendixen, C., Arnbjerg, J., Sorensen, C.M., Jensen, H.E., Shukri, N.M. and Thomsen, B. (2000) Abnormal growth plate function in pigs carrying a dominant mutation in type X collagen. *Mamm. Genome*, **11**, 1087–1092.
4. Bateman, J.F., Wilson, R., Freddi, S., Lamande, S.R. and Savarirayan, R. (2005) Mutations of *COL10A1* in Schmid metaphyseal chondrodysplasia. *Hum. Mutat.*, **25**, 525–534.
5. Chan, D. and Jacenko, O. (1998) Phenotypic and biochemical consequences of collagen X mutations in mice and humans. *Matrix Biol.*, **17**, 169–184.
6. Chan, D., Weng, Y.M., Graham, H.K., Sillence, D.O. and Bateman, J.F. (1998) A nonsense mutation in the carboxyl-terminal domain of type X collagen causes haploinsufficiency in schmid metaphyseal chondrodysplasia. *J. Clin. Invest.*, **101**, 1490–1499.
7. Bateman, J.F., Freddi, S., Nattrass, G. and Savarirayan, R. (2003) Tissue-specific RNA surveillance? Nonsense-mediated mRNA decay causes collagen X haploinsufficiency in Schmid metaphyseal chondrodysplasia cartilage. *Hum. Mol. Genet.*, **12**, 217–225.
8. Frischmeyer, P.A. and Dietz, H.C. (1999) Nonsense-mediated mRNA decay in health and disease. *Hum. Mol. Genet.*, **8**, 1893–1900.
9. Chan, D., Ho, M.S. and Cheah, K.S. (2001) Aberrant signal peptide cleavage of collagen X in Schmid metaphyseal chondrodysplasia.

Implications for the molecular basis of the disease. *J. Biol. Chem.*, **276**, 7992–7997.

10. Kwan, K.M., Pang, M.K., Zhou, S., Cowan, S.K., Kong, R.Y., Pfordte, T., Olsen, B.R., Sillence, D.O., Tam, P.P. and Cheah, K.S. (1997) Abnormal compartmentalization of cartilage matrix components in mice lacking collagen X: implications for function. *J. Cell. Biol.*, **136**, 459–471.

11. Chan, D., Freddi, S., Weng, Y.M. and Bateman, J.F. (1999) Interaction of collagen α1(X) containing engineered NC1 mutations with normal α1(X) *in vitro*. Implications for the molecular basis of schmid metaphyseal chondrodysplasia. *J. Biol. Chem.*, **274**, 13091–13097.

12. Marks, D.S., Gregory, C.A., Wallis, G.A., Brass, A., Kadler, K.E. and Boot-Handford, R.P. (1999) Metaphyseal chondrodysplasia type Schmid mutations are predicted to occur in two distinct three-dimensional clusters within type X collagen NC1 domains that retain the ability to trimerize. *J. Biol. Chem.*, **274**, 3632–3641.

13. McLaughlin, S.H., Conn, S.N. and Bulleid, N.J. (1999) Folding and assembly of type X collagen mutants that cause metaphyseal chondrodysplasia-type schmid. Evidence for co-assembly of the mutant and wild-type chains and binding to molecular chaperones. *J. Biol. Chem.*, **274**, 7570–7575.

14. Byers, P.H. (2002) Killing the messenger: new insights into nonsense-mediated mRNA decay. *J. Clin. Invest*, **109**, 3–6.

15. Wilson, R., Freddi, S., Chan, D., Cheah, K.S. and Bateman, J.F. (2005) Misfolding of collagen X chains harboring schmid metaphyseal chondrodysplasia mutations results in aberrant disulfide bond formation, intracellular retention, and activation of the unfolded protein response. *J. Biol. Chem.*, **280**, 15544–15552.

16. Chan, D., Weng, Y.M., Hocking, A.M., Golub, S., McQuillan, D.J. and Bateman, J.F. (1996) Site-directed mutagenesis of human type X collagen. Expression of α1(X) NC1, NC2, and helical mutations *in vitro* and in transfected cells. *J. Biol. Chem.*, **271**, 13566–13572.

17. McIntosh, I., Abbott, M.H., Warman, M.L., Olsen, B.R. and Francomano, C.A. (1994) Additional mutations of type X collagen confirm *COL10A1* as the Schmid metaphyseal chondrodysplasia locus. *Hum. Mol. Genet.*, **3**, 303–307.

18. Kaufman, R.J. (2002) Orchestrating the unfolded protein response in health and disease. *J. Clin. Invest.*, **110**, 1389–1398.

19. Gass, J.N., Gifford, N.M. and Brewer, J.W. (2002) Activation of an unfolded protein response during differentiation of antibody-secreting B cells. *J. Biol. Chem.*, **277**, 49047–49054.

20. Ma, Y., Brewer, J.W., Diehl, J.A. and Hendershot, L.M. (2002) Two distinct stress signaling pathways converge upon the CHOP promoter during the mammalian unfolded protein response. *J. Mol. Biol.*, **318**, 1351–1365.

21. Lee, K., Tirasophon, W., Shen, X., Michalak, M., Prywes, R., Okada, T., Yoshida, H., Mori, K. and Kaufman, R.J. (2002) IRE1-mediated unconventional mRNA splicing and S2P-mediated ATF6 cleavage merge to regulate XBP1 in signaling the unfolded protein response. *Genes Dev.*, **16**, 452–466.

22. Yoshida, H., Matsui, T., Yamamoto, A., Okada, T. and Mori, K. (2001) XBP1 mRNA is induced by ATF6 and spliced by IRE1 in response to ER stress to produce a highly active transcription factor. *Cell*, **107**, 881–891.

23. Karsenty, G. and Wagner, E.F. (2002) Reaching a genetic and molecular understanding of skeletal development. *Dev. Cell*, **2**, 389–406.

24. de Crombrugghe, B., Lefebvre, V. and Nakashima, K. (2001) Regulatory mechanisms in the pathways of cartilage and bone formation. *Curr. Opin. Cell Biol.*, **13**, 721–727.

25. Bogin, O., Kvansakul, M., Rom, E., Singer, J., Yayon, A. and Hohenester, E. (2002) Insight into Schmid metaphyseal chondrodysplasia from the crystal structure of the collagen X NC1 domain trimer. Structure (*Camb.*), **10**, 165–173.

26. Brass, A., Kadler, K.E., Thomas, J.T., Grant, M.E. and Boot-Handford, R.P. (1992) The fibrillar collagens, collagen VIII, collagen X and C1q complement proteins share a similar domain in their C-terminal non-collagenous regions. *FEBS Lett.*, **303**, 126–128.

27. Wilson, R., Freddi, S. and Bateman, J.F. (2002) Collagen X chains harboring Schmid metaphyseal chondrodysplasia NC1 domain mutations are selectively retained and degraded in stably transfected cells. *J. Biol. Chem.*, **277**, 12516–12524.

28. Wilson, R., Freddi, S., Chan, D., Cheah, K.S. and Bateman, J.F. (2005) Misfolding of collagen X chains harboring Schmid metaphyseal chondrodysplasia mutations results in aberrant disulfide bond formation, intracellular retention, and activation of the unfolded protein response. *J. Biol. Chem.*, **280**, 15544–15552.

29. Gow, A. and Sharma, R. (2003) The unfolded protein response in protein aggregating diseases. *Neuromol. Med.*, **4**, 73–94.

30. Kaufman, R.J., Scheuner, D., Schroder, M., Shen, X., Lee, K., Liu, C.Y. and Arnold, S.M. (2002) The unfolded protein response in nutrient sensing and differentiation. *Nat. Rev. Mol. Cell. Biol.*, **3**, 411–421.

31. Rutkowski, D.T., Arnold, S.M., Miller, C.N., Wu, J., Li, J., Gunnison, K.M., Mori, K., Akha, A.A., Raden, D. and Kaufman, R.J. (2006) Adaptation to ER stress is mediated by differential stabilities of pro-survival and pro-apoptotic mRNAs and proteins. *PLoS Biol.*, **4**, 2024–2041.

32. Shang, J. and Lehrman, M.A. (2004) Discordance of UPR signaling by ATF6 and Ire1p-XBP1 with levels of target transcripts. *Biochem. Biophys. Res. Commun.*, **317**, 390–396.

33. Yang, L., Carlson, S.G., McBurney, D. and Horton, W.E., Jr. (2005) Multiple signals induce endoplasmic reticulum stress in both primary and immortalized chondrocytes resulting in loss of differentiation, impaired cell growth, and apoptosis. *J. Biol. Chem.*, **280**, 31156–31165.

34. Ivkovic, S., Yoon, B.S., Popoff, S.N., Safadi, F.F., Libuda, D.E., Stephenson, R.C., Daluiski, A. and Lyons, K.M. (2003) Connective tissue growth factor coordinates chondrogenesis and angiogenesis during skeletal development. *Development*, **130**, 2779–2791.

35. Schroder, M., Clark, R., Liu, C.Y. and Kaufman, R.J. (2004) The unfolded protein response represses differentiation through the RPD3-SIN3 histone deacetylase. *EMBO J.*, **23**, 2281–2292.

36. Chan, D., Weng, Y.M., Golub, S. and Bateman, J.F. (1996) Type X collagen NC1 mutations produced by site-directed mutagenesis prevent *in vitro* assembly. *Ann. N.Y. Acad. Sci.*, **785**, 231–233.

37. Gordon, J.W. (1993) In Wassarman, P.M. and DePamphilis, M.L. (eds), *Guide to Techniques in Mouse Development*. Academic Press Inc., San Diego, Vol. 225, pp. 747–771.

38. Wai, A.W., Ng, L.J., Watanabe, H., Yamada, Y., Tam, P.P. and Cheah, K.S. (1998) Disrupted expression of matrix genes in the growth plate of the mouse cartilage matrix deficiency (cmd) mutant. *Dev. Genet.*, **22**, 349–358.

39. Roest, P.A., Roberts, R.G., Sugino, S., van Ommen, G.J. and den Dunnen, J.T. (1993) Protein truncation test (PTT) for rapid detection of translation-terminating mutations. *Hum. Mol. Genet.*, **2**, 1719–1721.

40. Bateman, J.F., Freddi, S., Lamande, S.R., Byers, P., Nasioulas, S., Douglas, J., Otway, R., Kohonen-Corish, M., Edkins, E. and Forrest, S. (1999) Reliable and sensitive detection of premature termination mutations using a protein truncation test designed to overcome problems of nonsense-mediated mRNA instability. *Hum. Mutat.*, **13**, 311–317.